

MID-INFRARED QUANTUM CASCADE LASERS

S.O. Edeagu

Abstract

Quantum cascade lasers (QCL) based on intersubband transitions operating at room temperature in the mid-infrared or 'molecular fingerprint' spectral region $(3.4-17 \ \mu m)$ have been found useful for several applications including environmental sensing, pollution monitoring, and medical applications. In this tutorial review we present an introductory overview of the design and development of mid-infrared quantum cascade lasers and their applications.

Keywords: laser, intersubband transitions, quantum cascade, mid-infrared, quantum well

1. Introduction

Semiconductor lasers have become ubiquitous devices in today's modern high-tech society. They can be found in familiar devices such as bar-code scanners used in supermarkets, laser printers in offices, compact disc and digital versatile disc (DVD) players at home and laser pointers used during presentations. They are widely used in industry for example, cutting and welding metals and other materials, in medicine for surgery, in optical communications, in optical metrology and in scientific research.

The laser is theoretically based on Einstein's classic paper of 1917, in which he introduced the concept of stimulated or induced emission of radiation [1]. The first demonstration of stimulated emission took place in 1954 when Townes and co-workers used a beam of ammonia (NH_3) gas, in a microwave device called the maser (*microwave amplification* by stimulated emission radiation) [2]. It generated a coherent source of microwaves at 23.87 GHz. In 1958, Schawlow and Townes proposed a theory extending stimulated emission to optical and infrared frequencies [4]. Two years later, the optical equivalent of the maser - the laser (light amplification by stimulated emission radiation) - was demonstrated by Maiman [5]. He used a three-level ruby laser emitting light of wavelength 693 nm.

The first theoretical understanding of the requirements for the realization of stimulated emission in a semiconductor was developed by Bernard and Duraffourg of the Centre National d'Etudes des Télécommunications (CNET), France and published in 1961 [6]. The equations derived by them became known as the Bernard-Duraffourg condition. In late 1962, the first reports of the operation of semiconductor injection lasers were published. The four independent groups were Hall and co-workers at the GE Research Lab, New York [7], Nathan and co-workers at the IBM T.J. Watson Research Center, New York [8], Holonyak and co-workers at the GE Advanced Semiconductor Lab, New York [9] and Quist and coworkers at Lincoln Lab, MIT [10]. These lasers were achieved using GaAs p-n junctions.

In 1994, a fundamentally different kind of laser diode known as the *quantum cascade laser* (QCL) emerged. During the last decade significant improvements made in quantum cascade lasers has led to its gradual emergence as the mid-infrared source of choice. The quantum cascade laser's unique properties, such as its small size, high output power, tunability of the emission wavelength, and ability to work in pulsed and continuous wave mode at room temperature, make it ideal for the remote sensing of environmental gases and pollutants.

2. Basic Concepts

Conventional semiconductor lasers operate via radiative recombination of an electron in the conduction band with a hole in the valence band (band-band transition or inter-band transition). The recombination generates a photon. Fig. 1 shows a schematic diagram of an interband transition. Due to the fact that two types of carriers, electron and holes, are involved, semiconductor lasers are also known as bipolar lasers. In contrast, the quantum cascade laser, makes

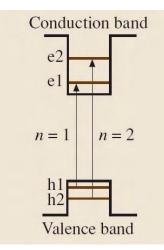


Figure 1: Interband optical transitions between confined states in a quantum well [13].

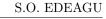
use of only a single carrier, the electron. The radiative recombination takes place within a single band between two bound states of a potential well (intraband transition or intersubband transition), as illustrated in Fig. 2. Through so-called electron recycling, a single electron generates multiple photons.

Quantum cascade lasers (QCLs) [14] are semiconductor lasers which rely on inter-subband transitions in a multiple quantum-well heterostructure. The transitions typically occur in the mid- and far-infrared spectral region. QCLs are based on two fundamental phenomena of quantum mechanics, namely *tunneling* and quantum confinement.

The original idea for creating the quantum cascade laser was first postulated in 1970 by two theoreticians, Kazarinov and Suris of the Ioffe Institute in Leningrad (now St. Petersburg) [15]. They proposed that one could obtain light amplification based on intersubband transitions in quantum wells electrically pumped by resonant tunneling. Their proposal came shortly after a seminal paper on the superlattice concept by Esaki and Tsu of the IBM Research Labs [16].

However due to the lack of appropriate technology in the 1970s, it took more than twenty years before the first quantum cascade laser was invented and demonstrated by the Bell Labs groups of Capasso and Cho in 1994 [14][17]. This achievement was largely made possible by the emergence of molecular beam epitaxy (MBE) as a practical crystal growth technology for quantum well heterostructures, largely pioneered by Cho at Bell Laboratories [18].

Quantum cascade lasers, also known as unipolar lasers, are designed by means of band-gap engineering [19]. The art of band-gap engineering enables one to engineer new materials by tuning their band gap. The first QCL was constructed from a concatenated series of quantum wells, using the GaAs/Al_xIn_{1-x}As



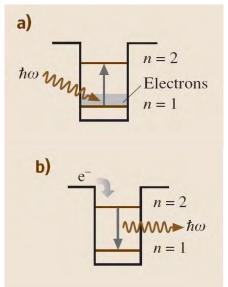


Figure 2: (a) Intersubband absorption in an n-type quantum well. (b) Intersubband emission following electron injection to a confined upper level in the conduction band [13].

material system lattice-matched to InP [14]. Over the years other material systems have been used to demonstrate QCLs. In 1998, Sirtori and coworkers used the GaAs/AlGaAs on GaAs material system [20]. Others include InAs/AlSb [21] [22] and InGaAs/AlAsSb [23]. These designed quantum well structures are grown by using thin-film crystal growth techniques such as molecular beam epitaxy (MBE) or metal-organic chemical vapor deposition (MOCVD) [18].

The design of a QCL consists of one basic structure called a *period* or *stage*, repeated multiple times (typically 25 to 75). Each period consists of an active region, where the optical transition takes place, and an relaxation/injector region, where the carriers can relax after having completed the optical transition. The active region is undoped and contains the quantum wells and barrier regions that support the electronic states while the relaxation/injector region is n-doped.

For the QCL invented by Faist et al. in 1994, the laser structure consisted of 25 stages with the $Al_{0.48}In_{0.52}As$ - $Ga_{0.47}In_{0.53}$ -As heterojunction material system lattice matched to InP [14]. Each of the periods consisted of four AlInAs barriers forming three GaInAs quantum wells and a digitally graded AlIn-GaAs region that is doped.

Under an applied bias (an applied electric field of 10^5 V/cm) the band edges of the quantum wells are slightly tilted forming a staircase structure. The carriers (electrons) are injected by resonant tunneling from the ground state of one active region to the upper laser level of the active region in the neighboring period.

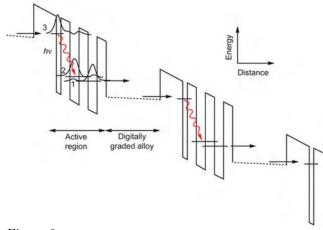


Figure 3: Schematic diagram of the conduction band for two periods of a quantum cascade laser with a quantum well active region [14]. The laser transition is indicated by the wavy arrows, and the electron flow by the straight arrows.

The electron drops in energy level emitting a photon in the process. As the electron moves from one stage to another, it emits multiple photons in a cascade process, as the electron remains inside the conduction band throughout its traversal of the active region.

3. Active Region Designs

There are two major designs for the active region of quantum cascade lasers: quantum-well active region and superlattice active region [11]. A third design, the so-called bound-to-continuum scheme, combines the features of the quantum-well QCL and the superlattice QCL. Various other designs for the QCL active region have been developed [24], which is far beyond the scope of this article.

3.1. Quantum-well active region

The quantum-well active region is based on the three-level laser system. The active region consists of three asymmetric coupled quantum wells (3QW), as shown in Fig. 3, and the laser transition takes place between the upper laser state (level 3) and the lower laser state (level 2) of the coupled system. Population inversion is only possible when the lifetime of the $3\rightarrow 2$ transition ($\tau_{32} \approx 1$ ps) is longer than the lifetime of level 2 ($\tau_2 \approx \tau_{21} \approx 0.1$ ps). Since $\tau_{32} \gg \tau_2$, laser action is possible.

3.2. Superlattice active region

The superlattice design [see Fig. 4.] was first proposed by Scamarcio in 1997 [26]. In this design, stimulated emission takes place between superlattice energy bands (mini-bands) separated by an energy gap called a *minigap*. Electrons are injected near the bottom of an upper miniband which then makes an optical transition to the top of the lower miniband. The

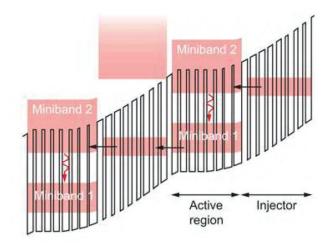


Figure 4: Schematic diagram of a superlattice QCL with a miniband-to-miniband radiative transition [26]. The laser transition is indicated by the wavy arrows, and the electron flow by the straight arrows.

laser frequency is thus determined by the height of the minigap. The extremely short electron lifetime (decay occurs rapidly) from the lower laser-level miniband makes this structure suitable for longer wavelengths $(\lambda \ge 10 \mu \text{m})$ [27–30].

3.3. Bound-to-continuum active region

In a bound-to-continuum design [31], transitions occur between a discrete upper state and a lower superlattice miniband. This design [see Fig. 5] combines the efficient electron injection into the upper laser level of the quantum-well design with the fast depopulation/electron extraction efficiency of the lower laser level of the superlattice design, thereby reducing the threshold and increasing the power.

The laser action involves transitions from a discrete upper state to a superlattice miniband. This design combines the efficient electron injection into the upper laser level of quantum-well QCLs with the fast depopulation of the lower laser level of superlattice QCLs, thereby reducing the threshold and increasing the power.

4. Quantum Cascade Laser Configurations

4.1. Fabry-Pérot quantum cascade lasers

This is the simplest of the quantum cascade lasers. An optical waveguide is first fabricated out of the quantum cascade material to form the gain medium. The ends of the crystalline semiconductor device are then cleaved (i.e. broken) to form two parallel mirrors on either end of the waveguide, thus forming a Fabry-Pérot resonator. The optical reflection (feedback) is provided by the borders of the resonator (facets). In

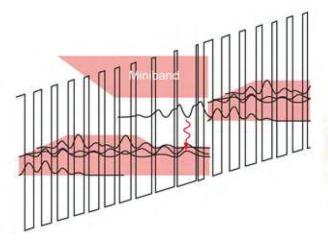


Figure 5: Schematic diagram of a bound-to-continuum QCL [31]. The laser transition is indicated by the wavy arrow.

many cases, the high refractive index difference between the semiconductor and the air is already sufficient, providing an optical reflection coefficient of about 30%. By additional facet coatings this coefficient can be tailored continuously between 0% (antireflection) and 100% (perfect reflection).

Fabry-Pérot quantum cascade lasers are capable of producing high powers [32], but are typically multimode at higher operating currents. The wavelength can be changed chiefly by changing the temperature of the QCL.

4.2. Distributed feedback quantum cascade lasers

QCLs have been touted as a source for numerous commercial applications, one of which is gas sensing applications, e.g. to detect very small concentrations of pollutants in air. These applications usually require single mode operation with good side-mode suppression ratio (SMSR)¹ which can be controlled and tuned over a certain wavelength range. This is usually achieved by introducing a distributed feedback (DFB) structure into the QCL active region [see Fig. 6].

Distributed feedback QCLs require a periodic modulation (i.e., a grating) of a material parameter (e.g., the refractive index or loss coefficient) to be integrated into the device. Repeated scattering from the firstorder grating favors one wavelength (the Bragg wavelength) and it is the grating period rather than the peak position of the gain spectrum that determines the single-mode emission wavelength.

DFB QCLs were first demonstrated in 1996 [34,35] and is based on the concept of distributed feedback

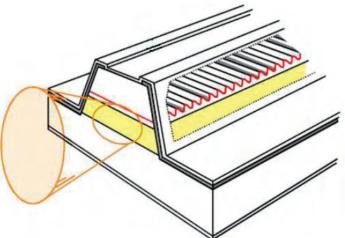


Figure 6: Schematic of a distributed feedback quantum cascade laser [33].

introduced in the early 1970s by Kogelnik and Shank [36].

4.3. External cavity quantum cascade lasers

Conventional quantum cascade lasers are at most only narrowly tunable. The DFB QCL does not provide a broadly tunable laser for the mid-IR. The range of wavelength tuning of the emitted laser radiation is limited by the limited tuning range of the distributed feedback structures. Typically the thermal tuning range of DFB QCLs is achieved by varying either the temperature of the chip or the laser injection current. By varying the injection current and/or temperature, the effective refractive index is modified which in turn changes the optical path length of the cavity and thus the emission wavelength. One of the disadvantages of such a thermal tuning is that it affects the effective gain of the QCL, which consequently causes a decrease of the output laser power with increasing temperature of the QCL chip. To overcome these drawbacks, the external cavity quantum cascade laser system was developed [37–39].

In the external cavity configuration, the QCL is coupled to an external cavity that incorporates a diffraction grating as a wavelength-selective element, which then provides frequency-selective optical feedback to the QCL via its antireflection-coated output facet. This concept of frequency selective feedback allows the laser to achieve narrow linewidth and remarkable tunability. Typically, such feedback is obtained through diffraction grating in either the Littrow or Littman-Metcalf configuration.

The most popular arrangement of an external cavity of a QCL, shown in Fig. 7, is based on the grating feedback in the Littrow configuration. The QCL chip is mounted on a thermoelectric (TE) cooler and has its front facet anti-reflection (AR) coated. In such

 $^{{}^{1}}SMSR = 10 \log_{10}(P_{1}/P_{2})$ where P_{1} and $P_{2} \leq P_{1}$ denote the output power of the two strongest modes in the optical spectrum. The SMSR for DFB QCLs readily reaches 30 dB, which qualifies them as 'single-mode' lasers.

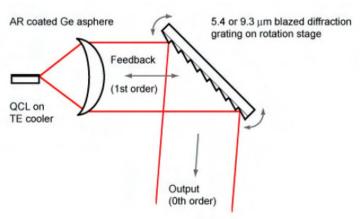


Figure 7: External-cavity setup (Littrow configuration).

configuration, the grating reflects back to the QCL the radiation in non-zero diffraction order (first-order feedback). The laser output coupling is performed through zero diffraction order of the grating.

5. Applications

The mid-infrared (MIR) spectral region, is sometimes called the *fingerprint region* of the electromagnetic spectrum, because most molecules have their fundamental vibrational-rotational absorption bands in this range. The MIR absorption spectrum is very specific to the structure of a particular molecule, allowing highly selective detection. In addition, since these absorption lines are very strong (several orders of magnitude stronger than the overtone and combination bands in the NIR), concentrations in the partsper-billion (ppb) to parts-per-trillion (ppt) ranges can be detected using relatively compact laser-based sensors. Fast, sensitive, and selective chemical sensors are needed in numerous applications. In industrial process control they are used for detection of contamination in semiconductor fabrication lines and for plasma monitoring, in law enforcement for drug and explosive detection, in automotive industry for engine exhaust analysis, in environmental science for pollution monitoring of important gas species (CO, CO_2 , CH_4 and CH_2O), in medical diagnostics for exhaled breath analysis (e.g. NO, CO, CO_2 , NH_3 and CS_2), and in homeland security for detection of chemical warfare agents.

Another interesting feature of the MIR are the *at-mospheric transmission windows* between 3 - 5 μ m and 8 - 12 μ m which enable free-space optical communications, remote sensing, and thermal imaging. High power lasers in the 3 - 5 μ m range will also enable the development of infrared counter-measures for home-land security.

6. Conclusion

In this paper, we have discussed the design and development of quantum cascade lasers in the midinfrared spectral range which have unique features that are well adapted for applications ranging from chemical sensing and detection, remote sensing to freespace optical communications.

References

- Einstein, A. Zur Quantentheorie der Strahlung (On the Quantum Theory of Radiation). *Phys. Z.*, Vol. 18, 1917, pp. 121-128.
- Gordon, J. P., Zeiger, H. J. and Townes, C. H. Molecular Microwave Oscillator and New Hyperfine Structure in the Microwave Spectrum of NH₃. *Phys. Rev.*, Vol. 95, Issue 1, 1954, pp. 282-284.
- Gordon, J. P., Zeiger, H. J. and Townes, C. H. The Maser - New Type of Microwave Amplifier, Frequency Standard, and Spectrometer. *Phys. Rev.*, Vol. 99, Issue 4, 1955, pp. 1264-1274.
- Schawlow, A. L. and Townes, C. H. Infrared and Optical Masers. *Phys. Rev.*, Vol. 112, Issue 6, 1958, pp. 1940-1949.
- Maiman, T. H. Stimulated Optical Radiation in Ruby. *Nature*, Vol. 187, Issue 4736, 1960, pp. 493-494.
- Bernard, M. G. A. and Duraffourg, G. Laser Conditions in Semiconductors. *Phys. Stat. Sol.*, Vol. 1, Issue 7, 1961, pp. 699-703.
- Hall, R. N., Fenner, G. E., Kingsley, J. D., Soltys, T. J. and Carlson, R. O. Coherent light emission from GaAs junctions. *Phys. Rev. Lett.*, Vol. 9, Issue 9, 1962, pp. 366-368.
- Nathan, M. I., Dumke, W. P., Burns, G., Dill, Jr., F. H. and Lasher, G. Stimulated emission of radiation from GaAs p-n junctions. *Appl. Phys. Lett.*, Vol. 1, Issue 3, 1962, pp. 62-64.
- Holonyak, Jr. N. and Bevacqua, S. F. Coherent (visible) light emission from Ga(As_{1-x}P_x) junctions. *Appl. Phys. Lett.*, Vol. 1, Issue 4, 1962, pp. 82-83.
- Quist, T. M., Rediker, R. H., Keyes, R. J., Krag, W. E., Lax, B., McWhorter, A. L. and Zeiger, H. J. Semiconductor maser of GaAs. *Appl. Phys. Lett.*, Vol. 1, Issue 4, 1962, pp. 91-92.
- Saleh, B. E. A. and Teich, M. C. Fundamentals of Photonics. Second Edition, John Wiley and Sons, New Jersey, 2007.
- Tittel, F. K., Richter, D. and Fried, A. Solid-State Mid-Infrared Laser Sources, Vol. 89 of Topics Appl. Phys. ch. Mid-Infrared Laser Applications in Spectroscopy. Sorokina, I. T. and Vodopyanov, K. L. (Eds.) Springer, Berlin, 2003, pp. 445-516.
- Fox, M. Springer Handbook of Electronic and Photonic Materials. Springer, New York, 2006, pp. 1021-1040.

- Faist, J., Capasso, F., Sivco, D. L., Sirtori, C., Hutchinson, A. L. and Cho, A. Y. Quantum Cascade Laser. *Science*, Vol. 264, Number 5158, 1994, pp. 553-556.
- Kazarinov, R. F. and Suris, R. A. Possibility of amplification of electromagnetic waves in a semiconductor with a superlattice. *Sov. Phys. Semicond.* (translated from *Fizika i Tekhnika Poluprovodnikov*, Vol. 5, pp. 797-800, 1971), Vol. 5, 1971, pp. 707-709.
- Esaki, L. and Tsu, R. Superlattice and Negative Differential Conductivity in Semiconductors. *IBM J. Res. Dev.*, Vol. 14, 1970, pp. 61-65.
- Capasso, F., Cho, A. Y., Faist, J., Hutchinson, A. L., Luryi, S., Sirtori, C. and Sivco, D. L. Unipolar semiconductor laser. U.S. Patent 5 457 709, 1995.
- Cho, A. Y. and Arthur, J. R. Molecular Beam Epitaxy. *Progress in Solid-State Chemistry*, Vol. 10, Issue 3, 1994, pp. 157-191.
- Capasso, F. Band-Gap Engineering: From Physics and Materials to New Semiconductor Devices. *Sci*ence, Vol. 235, Number 4785, 1987, pp. 172-176.
- Sirtori, C., Kruck, P., Barbieri, S., Collot, P., Nagle, J., Beck, M., Faist, J. and Oesterle, U. GaAs/Al_xGa_{1-x}As quantum cascade lasers. *Appl. Phys. Lett.*, Vol. 73, Issue 24, 1998, pp. 3486-3488.
- Ohtani, K. and Ohno, H. InAs/AlSb quantum cascade lasers operating at 10 µm. Appl. Phys. Lett., Vol. 82, Issue 7, 2003, pp. 1003-1005.
- Teissier, R., Barate, D., Vicet, A., Alibert, C., Baranov, A. N., Marcadet, X., Renard, C., Garcia, M., Sirtori, C., Revin, D. and Cockburn, J. Room temperature operation of InAs/AlSb quantum cascade lasers. *Appl. Phys. Lett.*, Vol. 85, Issue 2, 2004, pp. 167-169.
- Revin, D. G., Wilson, L. R., Zibik, E. A., Green, R. P., Cockburn, J. W., Steer, M. J., Airey, R. J. and Hopkinson, M. InGaAs/AlAsSb quantum cascade lasers. *Appl. Phys. Lett.*, Vol. 85, Issue 18, 2004, pp. 3992-3994.
- 24. Gmachl, C., Capasso, F., Sivco, D. L. and Cho, A. Y. Recent progress in quantum cascade lasers and applications. *Rep. Prog. Phys.*, Vol. 64, Number 11, 2001, pp. 1533-1601.
- Scarpa, G. Design and fabrication of Quantum Cascade Lasers. PhD thesis, Technical University of Munich, 2002.
- Scamarcio, G., Capasso, F., Sirtori, C., Faist, J., Hutchinson, A. L., Sivco, D. L. and Cho, A. Y. High-Power Infrared (8-Micrometer Wavelength) Superlattice Lasers. *Science*, Vol. 276, Number 5313, 1997, pp. 773-776.
- 27. Tredicucci, A., Gmachl, C., Capasso, F., Sivco, D. L., Hutchinson, A. L. and Cho, A. Y. Long wavelength superlattice quantum cascade lasers at $\approx 17 \mu m$. *Appl. Phys. Lett.*, Vol. 74, Issue 5, 1999, pp. 638-640.

- Tredicucci, A., Gmachl, C., Capasso, F., Hutchinson, A. L., Sivco, D. L. and Cho, A. Y. Single-mode surface-plasmon laser. *Appl. Phys. Lett.*, Vol. 76, Issue 16, 2000, pp. 2164-2166.
- Tredicucci, A., Gmachl, C., Wanke, M. C., Capasso, F., Hutchinson, A. L., Sivco, D. L., Chu, S. G. and Cho, A. Y. Surface plasmon quantum cascade lasers at λ ~ 19µm. Appl. Phys. Lett., Vol. 77, Issue 15, 2000, pp. 2286-2288.
- 30. Colombelli, R., Capasso, F., Gmachl, C., Hutchinson, A. L., Sivco, D. L., Tredicucci, A., Wanke, M. C., Sergent, A. M. and Cho, A. Y. Far-infrared surfaceplasmon quantum cascade lasers at 21.5 μm and 24 μm wavelengths. Appl. Phys. Lett., Vol. 78, Issue 18, 2001, pp. 2620-2622.
- Faist, J., Beck, M., Aellen, T. and Gini, E. Quantumcascade lasers based on a bound-to-continuum transition. *Appl. Phys. Lett.*, Vol. 78, Issue 2, 2001, pp. 147-149.
- 32. Slivken, S., Evans, A., David, J. and Razeghi, M. High-average-power, high-duty-cycle ($\lambda \sim 6\mu$ m) quantum cascade lasers. *Appl. Phys. Lett.*, Vol. 81, Issue 23, 2002, pp. 4321-4323.
- 33. Faist, J., Capasso, F., Sirtori, C., Sivco, D. L., Baillargeon, J. N., Hutchinson, A. L., Chu, S.-N. G. and Cho, A. Y. High power mid-infrared ($\lambda \sim 5\mu$ m) quantum cascade lasers operating above room temperature. *Appl. Phys. Lett.*, Vol. 68, Issue 26, 1996, pp. 3680-3682.
- 34. Faist, J., Gmachl, C., Capasso, F., Sirtori, C., Sivco, D. L., Baillargeon, J. N. and Cho, A. Y. Distributed feedback quantum cascade lasers. *Appl. Phys. Lett.*, Vol. 70, Issue 20, 1997, pp. 2670-2672.
- Gmachl, C., Faist, J., Baillargeon, J. N., Capasso, F., Sirtori, C., Sivco, D. L., Chu, S. N. G. and Cho, A. Y. Complex-coupled quantum cascade distributedfeedback laser. *IEEE Photon. Technol. Lett.*, Vol. 9, Issue 8, 1997, pp. 1090-1092.
- Kogelnik, H. and Shank, C. V. Coupled-Wave Theory of Distributed Feedback Lasers. J. Appl. Phys., Vol. 43, Issue 5, 1972, pp. 2327-2335.
- 37. Luo, G. P., Peng, C., Le, H. Q., Pei, S. S., Hwang, W.-Y., Ishaug, B., Um, J., Baillargeon, J. N. and Lin, C.-H. Grating-tuned external-cavity quantumcascade semiconductor lasers. *Appl. Phys. Lett.*, Vol. 78, Issue 19, 2001, pp. 2834-2836.
- Totschnig, G., Winter, F., Pustogov, V., Faist, J. and Mller, A. Mid-infrared external-cavity quantumcascade laser. *Opt. Lett.*, Vol. 27, Issue 20, 2002, pp. 1788-1790.
- Peng, C., Luo, G. and Le, H. Q. Broadband, continuous, and fine-tune properties of external-cavity thermoelectric-stabilized mid-infrared quantumcascade lasers. *Appl. Opt.*, Vol. 42, Issue 24, 2003, pp. 4877-4882.